Received: 11 November 2020 | Revised: 15 March 2021 | Accepted: 17 March 2021 | Accepted article online: 25 March 2021

DOI: 10.1002/pmic.202000283

Proteomics
Proteomics and Systems Biology

RESEARCH ARTICLE

Proteomic analysis of tyrosine phosphorylation induced by exogenous expression of oncogenic kinase fusions identified in lung adenocarcinoma

Sebastian A. Wagner[1,2] | **Pawel P. Szczesniak**[1] | **Andrea Voigt**[3] | **Justus F. Gräf**[3] | **Petra Beli**[3,4]

[1] Department of Medicine, Hematology/Oncology, Goethe University School of Medicine, Frankfurt, Germany

[2] German Cancer Consortium (DKTK), Heidelberg, Germany

[3] Institute of Molecular Biology (IMB), Mainz, Germany

[4] Institute of Developmental Biology and Neurobiology (IDN), Johannes Gutenberg University, Mainz, Germany

Correspondence
Sebastian A. Wagner, Department of Medicine, Hematology/Oncology, Goethe University School of Medicine, Frankfurt, Germany.
Email: swagner@med.uni-frankfurt.de

Funding information
Deutsche Forschungsgemeinschaft, Grant/Award Number: BE 5342/1-1; Else Kröner-Fresenius-Stiftung, Grant/Award Number: 2015_A124; Hessisches Ministerium für Wissenschaft und Kunst, Grant/Award Number: Ub-Net

Abstract

Kinase fusions are considered oncogenic drivers in numerous types of cancer. In lung adenocarcinoma 5–10% of patients harbor kinase fusions. The most frequently detected kinase fusion involves the Anaplastic Lymphoma Kinase (ALK) and Echinoderm Microtubule-associated protein-Like 4 (EML4). In addition, oncogenic kinase fusions involving the tyrosine kinases RET and ROS1 are found in smaller subsets of patients. In this study, we employed quantitative mass spectrometry-based phosphoproteomics to define the cellular tyrosine phosphorylation patterns induced by different oncogenic kinase fusions identified in patients with lung adenocarcinoma. We show that exogenous expression of the kinase fusions in HEK 293T cells leads to widespread tyrosine phosphorylation. Direct comparison of different kinase fusions demonstrates that the kinase part and not the fusion partner primarily defines the phosphorylation pattern. The tyrosine phosphorylation patterns differed between ALK, ROS1, and RET fusions, suggesting that oncogenic signaling induced by these kinases involves the modulation of different cellular processes.

KEYWORDS
ALK, fusion kinase, lung cancer, phosphoproteomics, RET, ROS1

1 | INTRODUCTION

In the last decade, advances in high-throughput sequencing technologies have enabled in-depth genetic characterization of tumors such as lung cancer and led to the discovery of numerous oncogenic drivers [1,2]. Gene fusions involving tyrosine kinases are found in diverse hematological and solid malignancies including acute lymphoblastic leukemia, chronic myeloid leukemia, lung cancer, and thyroid cancer [3–7]. Tyrosine kinase fusions result from genomic rearrangements such as chromosomal inversions or translocations and lead to expression of kinases that are constitutively activated through loss of inhibitory domains or artificial dimerization. Importantly, oncogenic tyrosine kinase fusions are an attractive target for cancer therapy and multiple kinase inhibitors have been approved for the treatment of patients harboring specific kinase fusions [8].

Approximately 5–10% patients with lung adenocarcinoma (LADC) harbor oncogenic tyrosine kinase fusions. Oncogenic tyrosine kinase fusions are primarily detected in young never-smokers and rarely co-occur with other known drivers such as pathogenic EGFR or KRAS variants [9]. Kinase fusions involving Anaplastic Lymphoma Kinase (ALK) are found in 3–6% of LADC patients and represent the most frequently identified kinase fusions in LADC. In the majority of cases, ALK is fused

C-terminally to the Echinoderm Microtubule-associated protein-Like 4 (EML4). A number of different breakpoints have been reported but, in all cases, the EML4 part retains its coil-coiled domain that mediates dimerization of the EML4-ALK protein and thereby leads to constitutive activation of the kinase [10]. In rare cases, fusions of ALK with another microtubule-associated protein Kinesin-1 heavy chain (KIF5B) have been reported. As in case of EML4-ALK, the coiled-coil domain of KIF5B mediates dimerization and leads to constitutive activation of the KIF5B-ALK fusion protein [11].

In addition to ALK fusions, fusions of the tyrosine kinases Proto-oncogene tyrosine protein kinase receptor Ret and Proto-oncogene tyrosine kinase ROS1 have been described in LADC [12, 13]. KIF5B-RET fusions have been identified in 1–2% of LADC patients. Functional investigations suggest that the kinase domain of RET is constitutively activated by artificial dimerization as in case of EML4- and KIF5B-ALK. More recently, fusion proteins involving ROS1 have been described in LADC. Kinase fusions involving ROS1 can be identified in 1–2% of patients LADC. In most cases ROS1 is C-terminally fused to the transmembrane protein CD74. However, a number of other fusion partners including SDC4, EZR, CCDC6, and SLC34A2 have been identified [14]. The activation mechanism of ROS1 kinase fusions is not yet completely understood, but it is likely that the kinase activation occurs through artificial dimerization. Targeted therapies against constitutively active tyrosine kinase fusions involving ALK, ROS1, and RET have proven effective for the treatment of LADC [15–19].

Mass spectrometry (MS)-based proteomics is a powerful approach to study phosphorylation-dependent cellular signaling in physiology and disease [20]. Large scale identification of tyrosine phosphorylation sites can be achieved by enrichment of tyrosine phosphorylated peptides using specific antibodies followed by their identification using high performance liquid chromatography tandem mass spectrometry (HPLC-MS/MS) [21–23]. Previous MS-based proteomics studies have delivered important insights into tyrosine phosphorylation-dependent signaling after growth factor stimulation. In addition, phosphoproteomics combined with kinase inhibition revealed protein substrates of kinases functioning in diverse cellular processes [24–29]. Rikova et al. reported in 2007 a comprehensive phosphoproteomic profiling of 41 NSCLC cell lines and over 150 NSCLC tumors expressing different oncogenic kinases [30]. However, to date a systematic, quantitative and comparative proteomic analysis of the phosphorylation signaling induced by different oncogenic tyrosine kinase fusions in a controlled cellular model system has not been performed. In this study, we employed quantitative phosphoproteomics based on stable isotope labelling with amino acids in cell culture (SILAC) to characterize tyrosine phosphorylation-dependent signaling that is induced downstream of oncogenic kinase fusions. To this end, kinase fusions involving ALK, ROS1, and RET frequently found in LADC were investigated. We found that exogenous expression of ALK, ROS1, and RET oncogenic fusions in HEK 293T cells results in widespread tyrosine phosphorylation. Quantitative comparison of the signaling downstream of different kinases and their fusion partners demonstrated that the kinase and not the fusion partner primarily defines to the observed phosphorylation patterns. Tyrosine phosphorylation patterns differed between ALK, ROS1, and RET fusions, suggesting that oncogenic signaling induced by these kinases involves the modulation of different cellular signaling processes.

Significance Statement

Kinase fusions are oncogenic drivers in lung adenocarcinoma and specific inhibition of kinase fusions by small molecules has proven effective for treatment. Despite this importance, the phosphorylation patterns induced by different oncogenic kinase fusions were not systematically investigated. In this study, we employed quantitative MS-based proteomics to comparatively analyze the phosphorylation patterns induced by exogenous expression of the oncogenic tyrosine kinase fusions EML4-ALK, KIF5B-ALK, KIF5B-RET, CD74-ROS1, and SDC4-ROS1 that are frequently found in patients with LADC. Our analyses demonstrate that all investigated kinase fusions induce widespread tyrosine phosphorylation and reveal that the kinase part primarily defines the induced phosphorylation patterns. However, we could also identify phosphorylation events that are likely specific to the fusion partner and might contribute to the subtle phenotypical differences observed in clinical trials. The acquired phosphoproteomics dataset might serve as a useful resource for future studies focused on the effects of kinase fusions in lung adenocarcinoma.

2 | MATERIAL AND METHODS

2.1 | Cell culture

Human embryonic kidney (HEK-293T) cells were obtained from ATCC and cultured in D-MEM medium supplemented with 10% fetal bovine serum, L-glutamine, penicillin, and streptomycin. For SILAC labeling, cells were cultured in media containing either L-arginine and L-lysine, L-arginine (13C6), and L-lysine (2H4) or L-arginine (13C6 15N4) and L-lysine (13C6 15N2) (Cambridge Isotope Laboratories) as described previously [31]. All cells were cultured at 37°C in a humidified incubator containing 5% CO_2.

2.2 | Cell lysis

Cells were washed with ice-cold phosphate buffered saline and lysed in modified RIPA buffer (50 mM Tris pH 7.5, 150 mM NaCl, 1 mM EDTA, 1% NP-40, 0.1% sodium deoxycholate) supplemented with protease inhibitors (Protease inhibitor cocktail, Sigma), 1 mM sodium orthovanadate, 5 mM β-glycerophosphate, 5 mM sodium fluoride. Lysates were cleared by centrifugation at 16,000 × g for 15 min and pro-

tein concentrations were estimated using QuickStart Bradford Protein assay (BioRad).

2.3 | MS sample preparation

Proteins were precipitated in fourfold excess of ice-cold acetone and subsequently redissolved in denaturation buffer (6 M urea, 2 M thiourea in 10 mM HEPES pH 8.0). Cysteines were reduced with 1 mM dithiothreitol and alkylated with 5.5 mM chloroacetamide. Proteins were digested with endoproteinase Lys-C (Wako Chemicals) and sequencing grade modified trypsin (Sigma). Protease digestion was stopped by addition of TFA to 0.5% and precipitates were removed by centrifugation. Peptides were purified using reversed-phase Sep-Pak C18 cartridges (Waters) and eluted in 50% acetonitrile. For the enrichment of tyrosine phosphorylated peptides, 5 mg of peptides were concentrated and redissolved in immunoprecipitation buffer (10 mM sodium phosphate, 50 mM sodium chloride in 50 mM MOPS pH 7.2). Precipitates were removed by centrifugation. Modified peptides were enriched using phosphotyrosine antibody resin (P-Tyr-1000, Cell Signaling Technology). Peptides were incubated with the antibodies for 4 h at 4 °C on a rotation wheel. Beads were washed three times in ice-cold immunoprecipitation buffer followed by three washes in water. The enriched peptides were eluted with 0.15% trifluoroacetic acid in water, fractionated in four fractions using micro-column-based SCX and desalted on reversed phase C18 StageTips [32].

2.4 | MS analysis

Peptide fractions were analyzed on a quadrupole Orbitrap mass spectrometer (Q Exactive Plus, Thermo Scientific) equipped with a UHPLC system (EASY-nLC 1000, Thermo Scientific) as described [33]. Peptide samples were loaded onto C18 reversed phase columns (15 cm length, 75 μm inner diameter, 1.9 μm bead size) and eluted with a linear gradient from 8 to 40% acetonitrile containing 0.1% formic acid in 2 h. The mass spectrometer was operated in data dependent mode, automatically switching between MS and MS2 acquisition. Survey full-scan MS spectra (m/z 300–1650) were acquired in the Orbitrap. The ten most intense ions were sequentially isolated and fragmented by higher energy C-trap dissociation (HCD) [34]. Peptides with unassigned charge states, as well as with charge states less than +2 were excluded from fragmentation. Fragment spectra were acquired in the Orbitrap mass analyzer.

2.5 | Peptide identification

Raw data files were analyzed using MaxQuant (development version 1.5.2.8) [35]. Parent ion and MS2 spectra were searched against a database containing 88,473 human protein sequences obtained from the UniProtKB released in December 2016 using Andromeda search engine [36]. Spectra were searched with a mass tolerance of 6 ppm in MS mode, 20 ppm in HCD MS2 mode, strict trypsin specificity and allowing up to three miscleavages. Cysteine carbamidomethylation was searched as a fixed modification, whereas protein N-terminal acetylation, methionine oxidation, and phosphorylation of serine, threonine, and tyrosine were searched as variable modifications. Site localization probabilities were determined by MaxQuant using the PTM scoring algorithm as described previously [35, 37]. The dataset was filtered based on posterior error probability to arrive at a false discovery rate (FDR) below 1% estimated using a target-decoy approach [38].

2.6 | Data analysis

Statistical analysis was performed using the R software environment. To identify significantly regulated phosphorylation sites a moderated T test (limma) was employed [39]. Only sites with a FDR-adjusted p value ≤ 0.01 were considered regulated. Kinase activities were estimated using the KSEA algorithm [40] and the R implementation of the KSEA App [41]. Kinase-Substrate annotations were obtained from PhosphoSitePlus (PSP) [42] and from the NetworKIN database [43]. The analysis was performed with a minimum NetworKIN score of 5 for upregulated and downregulated phosphorylation sites with a p value ≤ 0.05. Phosphosite-specific signature analysis was performed using PTM-SEA [44]. As input data p values generated during statistical analysis were transformed and multiplied by the sign of the averaged $\log_2$-transformed fold changes. As identifier for the phosphorylation sites the flanking sequence (+/- 7 amino acids) was used. PTM-SEA analysis was performed in R. 'PTM site-specific phosphorylation signatures of kinases, perturbations and signaling pathways' (PTMsigDB) was used as reference database. Minimal overlap between reference data and input data was set to 3.

2.7 | SDS-PAGE and Western blotting

Proteins were resolved on 4–12% gradient SDS-PAGE gels (NuPAGE Bis-Tris Precast Gels, Life Technologies) and transferred onto nitrocellulose membranes. Membranes were blocked using 10% skimmed milk solution in PBS supplemented with 0.1% Tween-20. For detection of FLAG-tagged kinase fusion anti-FLAG clone M2 (Sigma Aldrich) was used. Secondary antibodies coupled to horseradish peroxidase (Jackson ImmunoResearch Laboratories) were used for immunodetection. The detection was performed with SuperSignal West Pico Chemiluminescent Substrate (Thermo Scientific).

2.8 | Immunofluorescence and confocal microscopy

Cells were washed three times with PBS before fixation using 4% PFA solution in PBS containing Hoechst dye (5 μg/mL) for 15 min. After blocking and permeabilization in 0.2% BSA, 0.1% Triton X-100 in PBS for 15 min, cells were stained with anti-FLAG clone M2 (Sigma Aldrich) antibody for 1 h. Cells were then incubated with Alexa Fluor

TABLE 1 Oncogenic tyrosine kinase fusions investigated in this study

Name	Fusion partner	Last exon	Kinase part	First exon	Samples with exact same fusion	Samples with same fusion partner/kinase	Detection frequency in lung cancer	Detection frequency in other cancers
EML4-ALK	r.1_1751	13	r.4080_6220	20	175	711	7.19%	1.76% (Thyroid)
KIF5B-ALK	r.1_3219	24	r.4080_6220	20	4	10	0.48%	
KIF5B-RET	r.1_2183	15	r.2369_5659	12	36	62	1.52%	2.63% (Skin)
CD74-ROS1	r.1_627	6	r.5757_7435	34	33	39	2.32%	
SDC4-ROS1	r.1_239	2	r.5448_7435	32	3	5	0.76%	

For fusion partner and kinase part the involved regions are indicated. In addition, the frequency of the detection in lung cancer and other cancer types is indicated. The data provided here was extracted from the COSMIC database. The following reference sequences were used: ENST00000389048.7(ALK), ENST00000355710.7(RET), ENST00000368508.7(ROS1), ENST00000318522.9(EML4), ENST00000302418.4(KIF5B), ENST00000009530.11 (CD74), ENST00000372733.3 (SDC4).

488 goat anti-mouse IgG (1:1000 dilution in 1% BSA, Life Technologies) and mounted with fluorescent mounting medium (Dako). Images were acquired with a TCS SP5 confocal microscope (Leica) using a 63× oil objective (NA 1.4), fluorescence excitation with an argon-ion laser (488 nm) and constant imaging and detection settings.

3 | RESULTS AND DISCUSSION

3.1 | Cloning and expression of ALK, RET, and ROS1 kinase fusions

Oncogenic kinase fusions involving ALK, RET, and ROS1 are frequently found in patients with LADC. We employed the COSMIC database [45] to identify the most frequently observed fusion partners and breakpoints of the tyrosine kinases ALK, RET, and ROS1 (Figure 1A and Table 1). DNA sequences encoding kinases and fusion partners were obtained, relevant sequences were amplified by PCR and assembled into the pENTR1A vector using homology-based cloning. After sequence verification, the coding sequences of all kinase fusions were transferred into a custom Gateway compatible mammalian expression vector including an N-terminal FLAG-Strep tag for detection by western blotting. We transfected all DNA constructs into HEK 293T cells and analyzed their expression by western blotting with FLAG antibodies which confirmed that all kinase fusions were expressed and migrated at the expected size (Figure 1B).

To verify that the expressed kinase fusions are active in vivo we detected tyrosine phosphorylation using specific antibodies (pY-1000) in control cells transfected with the empty vector and in cells expressing the kinase fusions. We could observe a strong signal only in cells expressing the kinase fusions, indicating that the kinase fusions are active (Figure 1C).

It has been previously reported that the kinase fusions investigated in this study localize to different cellular compartments [9, 11, 46, 47]. To verify that the generated constructs retain these properties in our cellular system, we assessed the localization of the kinase fusions by immunofluorescence. We observed a cytoplasmic staining in case of EML4-ALK, KIF5B-ALK, and KIF5B-RET. The ROS1 fusions CD74-ROS1 and SDC4-ROS1 localized at the plasma membrane. These findings are in line with previous studies that have reported a distinct subcellular localization of ROS1 fusions compared to ALK and RET tyrosine kinase fusions in cancer samples and indicate that exogenous expression does not interfere with the localization (Figure 1D).

3.2 | Oncogenic kinase fusions induce widespread tyrosine phosphorylation

To investigate the effect of the oncogenic kinase fusions on the cellular phosphorylation patterns, we employed quantitative mass spectrometry (MS)-based proteomics. To this end, HEK 293T cells were metabolically labeled using SILAC. Subsequently, the labeled cells were transfected with the DNA constructs encoding the kinase fusions. After 48 h, cells were harvested and lysed to extract cellular proteins. Proteins were digested into peptides and peptides phosphorylated on tyrosine residues were specifically enriched using phosphotyrosine antibodies. The enriched peptide fractions were fractionated using strong cation exchange chromatography and analyzed by liquid chromatography-tandem mass spectrometry (LC-MS/MS). Raw data was analyzed with the MaxQuant software package. All experiments were carried out in triplicate to achieve robust quantification and to permit statistical analysis (Figure 2A and B). In total, we quantified 4634 tyrosine phosphorylation sites in these experiments (Figure S1A). Out of these tyrosine phosphorylation sites, 635 were quantified in at least two replicates across all experiments (Figure S1B). Similarity analysis and clustering of the normalized ratios confirmed a good reproducibility across biological replicates (Figure S1C).

To assess how the expression of the oncogenic fusions affects cellular tyrosine phosphorylation, we plotted the SILAC ratio distribution for each investigated kinase fusion. The analysis showed an increase in tyrosine phosphorylation that affected a large fraction of all quantified phosphorylation sites, demonstrating that expression of oncogenic fusions globally perturbs cellular signaling. The mean $\log_2$ SILAC ratio was nearly identical for all kinase fusions and ranged between 3.08 and 3.16 (Figure 2C). To identify significantly upregulated phosphorylation sites, we applied a moderated T test (limma algorithm) to the phosphorylation site dataset. Sites with a FDR-adjusted p value ≤ 0.01 were considered regulated. The fraction of upregulated sites

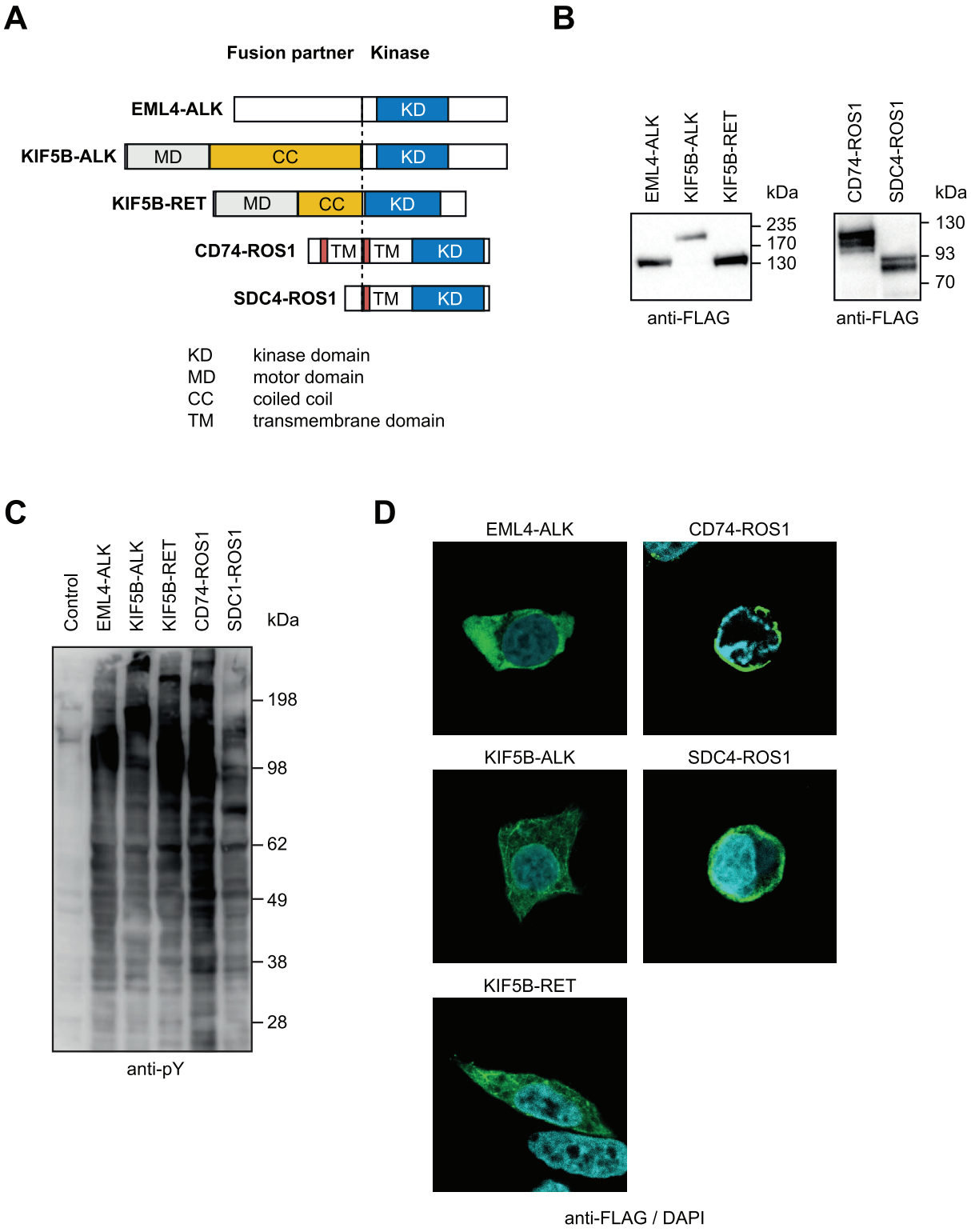

FIGURE 1 Oncogenic tyrosine kinase fusions investigated in this study. (A) Schematic representation of the domains of the investigated oncogenic tyrosine kinase fusions. (B) Validation of the kinase fusion expression by western blotting. HEK 293T cells were transfected with indicated kinase fusions and protein lysates were prepared 48 h after transfection. Proteins were separated by SDS-PAGE and kinase fusions were detected using FLAG antibodies. (C) Expression of kinase fusions leads to tyrosine phosphorylation of cellular proteins. HEK 293T cells were transfected with indicated kinase fusions and protein lysates were prepared 48 h after transfection. Proteins were separated by SDS-PAGE and tyrosine phosphorylation was detected by western blotting. (D) Subcellular localization of kinase fusions. HEK 293T cells were transfected with indicated kinase fusions and fixed 48 h after transfection. Localization of kinase fusions was monitored by immunofluorescence and confocal microscopy

A

Experiment	SILAC state		
	Light	Medium	Heavy
1	Control	CD74-ROS1	SDC4-ROS1
2	Control	KIF5B-ALK	KIF5B-RET
3	Control	EML4-ALK	KIF5B-ALK

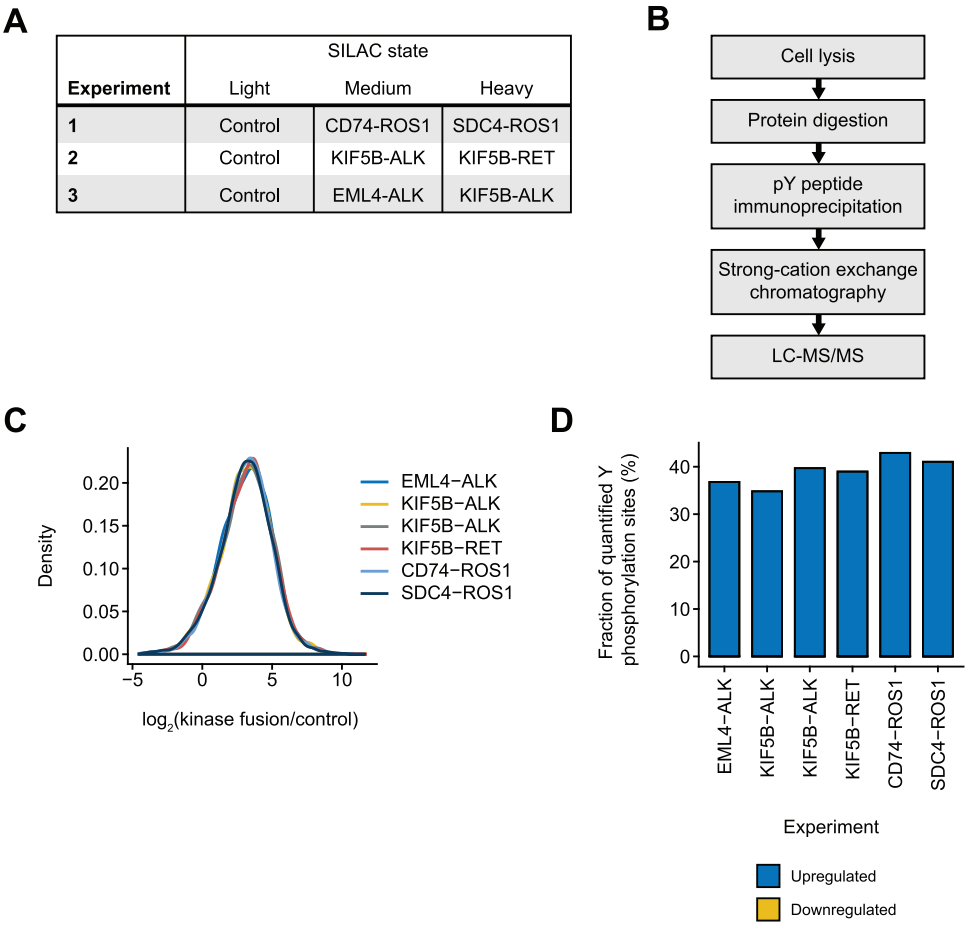

FIGURE 2 Expression of oncogenic tyrosine kinase fusions induces widespread tyrosine phosphorylation. (A) Schematic overview of the SILAC-based experimental setup used to compare tyrosine phosphorylation patterns in cells expressing different kinase fusions. Each experiment was performed in biological triplicate. (B) Schematic overview of the workflow used for enrichment and fractionation of tyrosine phosphorylated peptides from cells expressing kinase fusions. (C) SILAC ratio distribution of all quantified tyrosine phosphorylation sites. Expression of oncogenic tyrosine kinase fusions leads to increased phosphorylation of almost all quantified tyrosine phosphorylation sites. (D) The bar plot shows the fraction of upregulated and downregulated phosphorylation sites quantified from cells expressing different kinase fusions

ranged from 34.8% (for KIF5B-ALK) to 42.9% (for CD74-ROS1). Only few sites showed a significant downregulation upon overexpression of the kinase fusions (Figure 2D).

3.3 | Cellular phosphorylation patterns are primarily determined by the kinase in the fusion protein

To investigate the differences/similarities between the phosphorylation patterns induced by the kinase fusions, we performed multidimensional scaling based on the SILAC ratios. The analysis showed a clear separation of the fusion proteins comprising the kinases ALK, RET, and ROS1 (Figure 3A). In case of ALK, the analysis also allowed to distinguish between the different fusion partners EML4 and KIF5B, suggesting an impact of the fusion partner EML4 and KIF5B on the induced tyrosine phosphorylation patterns. The ROS1 fusions CD74-ROS1 and SDC4-ROS1 induced nearly identical phosphorylation patterns (Figure 3A). Hierarchical clustering of the phosphoproteomics data showed a similar result with oncogenic kinases containing ALK, ROS1 or RET clustering together irrespective of the investigated fusion partner (Figure 3B). Kinase-Substrate Enrichment Analysis (KSEA) confirmed prominent activation of the exogenously expressed kinases in the cells. Notably, we could also observe strong activation of several other kinases (PDGFRA, MST1R, FLT3, ERBB3, ERBB4, JAK2, and MET) in cells expressing KIF5B-RET and to a lower extend in cells expressing EML4—ALK and CD74—ROS1 (Figure 3C).

3.4 | ALK, RET, and ROS1 fusions activate different cellular signaling pathways

We subsequently performed annotation enrichment analysis to identify biological processes that are regulated by phosphorylation after overexpression of the investigated fusion kinases as well as to define the affected cellular compartments. To this end, annotations from the GO Ontology and the Reactome pathway database were employed. The analysis revealed that phosphorylation induced by all investi-

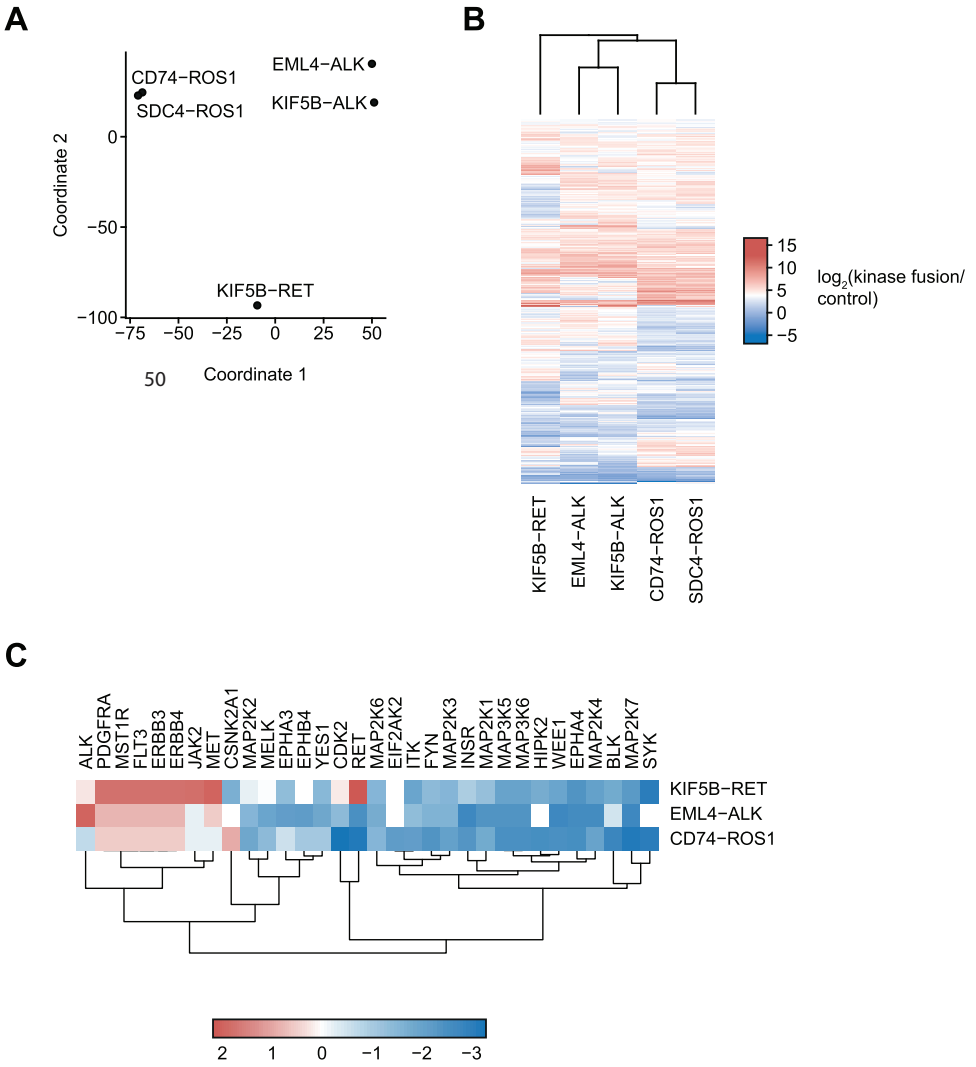

FIGURE 3 The kinase part primarily contributes to the cellular phosphorylation patterns induced by different kinase fusions. (A) Multidimensional scaling based on the SILAC ratios shows clear separation of fusion proteins containing different tyrosine kinases ROS1, ALK, and RET. (B) Hierarchical clustering of the phosphoproteomics data also allows separation of kinase fusions containing ROS1, ALK, and RET. (C) Kinase-Substrate Enrichment Analysis (KSEA) shows activation of the respective kinases in cells expressing KIF5B-RET, EML4—ALK, and CD74—ROS1

gated oncogenic kinases regulates RNA metabolism including mRNA splicing and translation initiation complex formation (Figure 4A, B, and C). In addition, expression of all kinases led to phosphorylation of proteins involved in cell cycle progression ("Regulation of PLK1 activity at G2/M transition"). Interestingly, a number of biological processes were regulated by only a specific kinase fusion either involving ALK, ROS1, or RET, suggesting that different fusions also regulate specific pathways (Figure 4A, B and C). For instance, expression of RET fusions led to specific phosphorylation of proteins involved in MHC class II antigen presentation (Figure 4A). Expression of ROS1 fusions led to the phosphorylation of proteins involved in RNA processing including 'Processing of Capped Intron-Containing Pre-mRNA' and 'Nonsense Mediated Decay enhanced by the Exon Junction Complex' as well as 'RHO GTPases Activate Formins' (Figure 4C, Figure S2B). In addition, the fusion partner showed an effect on the signaling activated downstream of ROS1: expression of SDC4-ROS1 resulted in phosphorylation of proteins involved in 'Prefoldin mediated transfer of substrate to CCT/TriC' (Figure S2B). In case of the KIF5B fusions KIF5B-ALK and KIF5B-RET, the Reactome term 'Kinesins' was significantly enriched, demonstrating that these kinase fusions lead to increased phosphorylation of KIF5B and other kinesins (Figure 4A). PTM Signature Enrichment Analysis (PTM-SEA) did not yield significantly enriched terms (Figure 4D).

3.5 | Kinase fusions lead to phosphorylation of fusion partners and interacting proteins

The annotation enrichment analysis suggested that kinase fusions comprising KIF5B induce tyrosine phosphorylation of KIF5B itself and

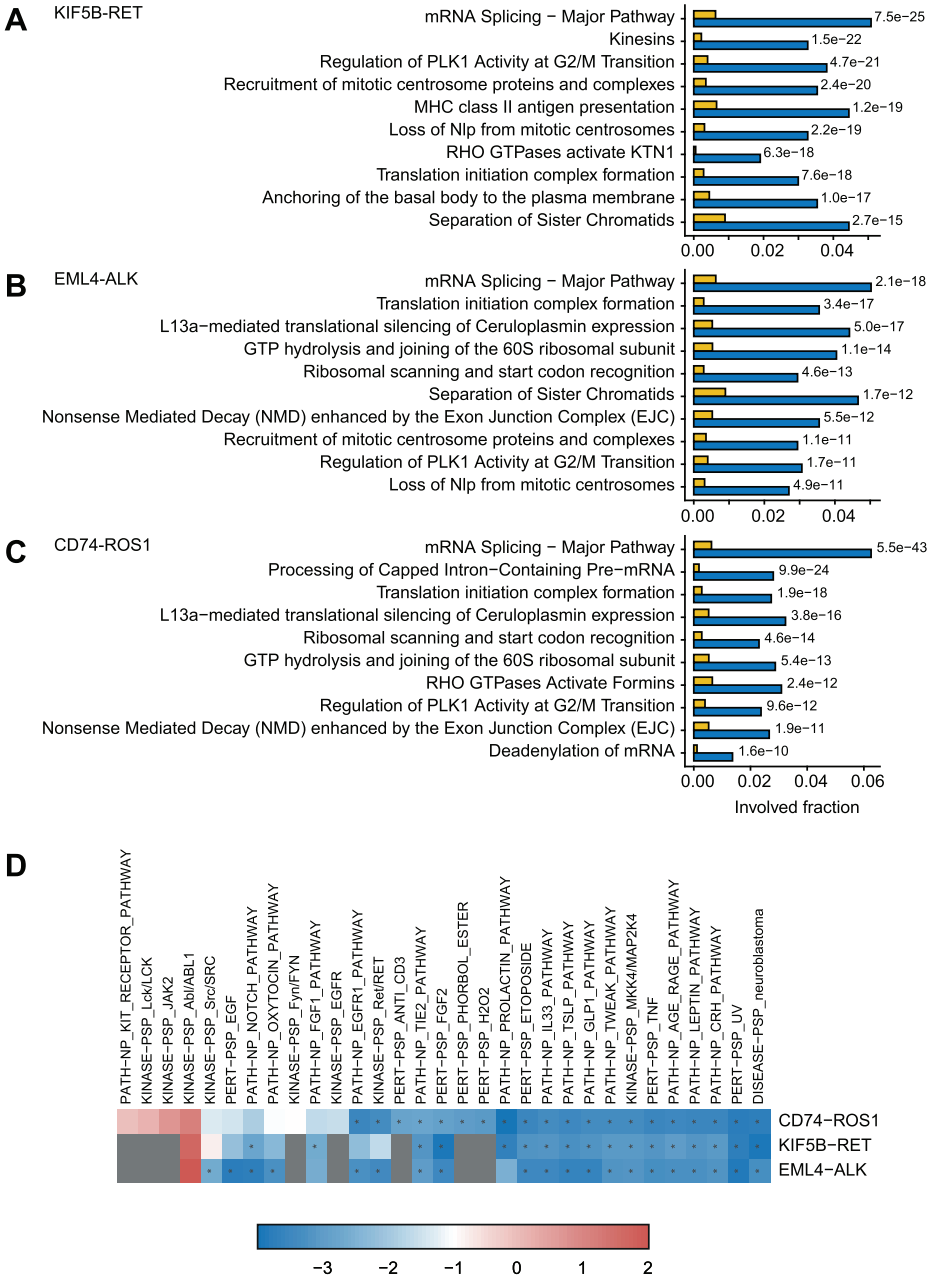

FIGURE 4 Biological processes regulated by different kinase fusions. (A) Gene Ontology (GO) terms significantly enriched among proteins with significantly upregulated tyrosine phosphorylation sites in cells expressing KIF5B-RET. The significance of the enrichment of a specific term was determined using Fisher's exact test. *p* values were corrected for multiple hypotheses testing using the Benjamini and Hochberg FDR. (B) Gene Ontology (GO) terms significantly enriched among proteins with significantly upregulated tyrosine phosphorylation sites in cells expressing EML4-ALK. (C) Gene Ontology (GO) terms significantly enriched among proteins with significantly upregulated tyrosine phosphorylation sites in cells expressing CD74-ROS1. (D) PTM Signature Enrichment Analysis (PTM-SEA)

possibly other kinesins. To investigate this finding in detail, we plotted the SILAC ratio of all phosphorylation sites on kinesin proteins. Indeed, we could confirm that multiple sites on KIF5B as well as on KIF5C were significantly phosphorylated after expression of KIF5B containing fusions, which was not observed in case of kinase fusions with other fusion partners. In addition to KIF5B, we also found an increase in phosphorylation of several other factors such as NEFM exclusively in case of KIF5B fusions (Figure 5A).

3.6 | ALK, RET, and ROS1 kinase fusions activate STAT signaling

The STAT signaling pathway has been previously identified as one of the signaling pathways mediating the oncogenic effect of ALK [48], RET [49], and ROS1 [50], fusion proteins. To gain further insights into the activation of the STAT transcription factors in cells expressing different kinase fusions, we investigated the phosphorylation of STAT

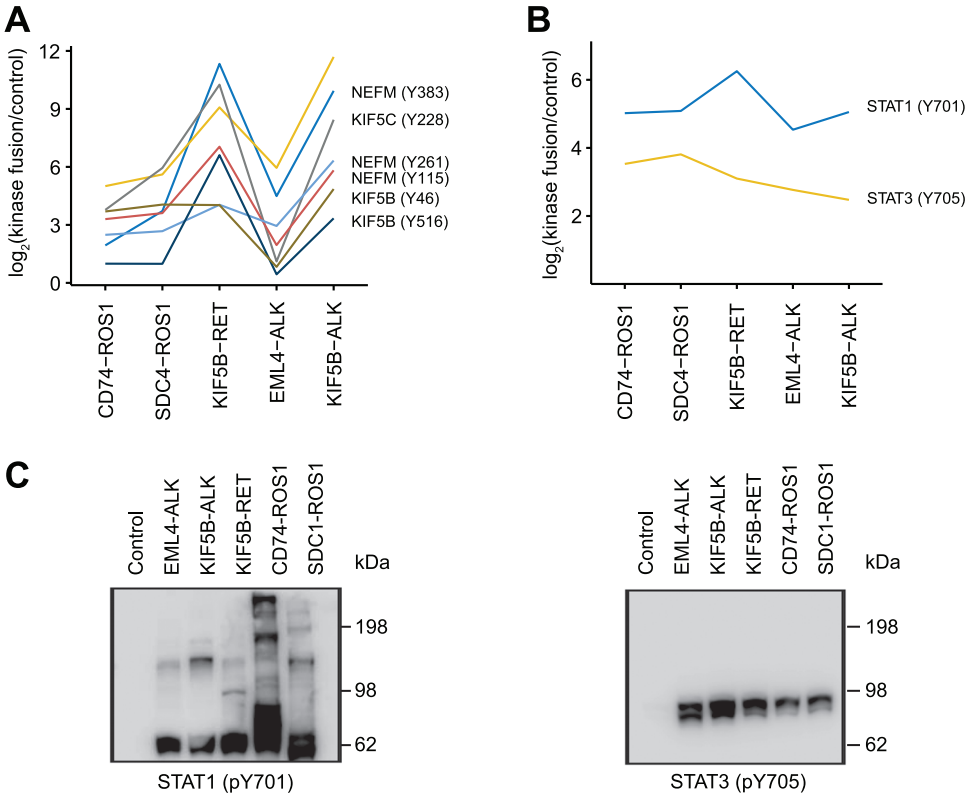

FIGURE 5 Phosphorylation of downstream effectors. (A) Line plots show the logarithmized SILAC ratios quantified for indicated tyrosine phosphorylated peptides in cells expressing different kinase fusions. (B) Line plots show the logarithmized SILAC ratios quantified for indicated tyrosine phosphorylated peptides in cells expressing different kinase fusions. (C) Expression of kinase fusions leads to tyrosine phosphorylation of STAT proteins. HEK 293T cells were transfected with indicated kinase fusions and protein lysates were prepared 48 h after transfection. Proteins were separated by SDS-PAGE and tyrosine phosphorylation was detected using the indicated antibodies

proteins. Our data shows a strong phosphorylation of STAT1 Y701 that is induced by all investigated kinases (Figure 5B and C). STAT1 Y701 is known to be phosphorylated in cells upon interferon stimulation and promotes dimerization and subsequent translocation to the nucleus [51, 52]. We also identified an increase in phosphorylation of Y705 on STAT3 in all kinase fusions (Figure 5B and C). Phosphorylation of this site was demonstrated to increase the transcriptional activity of STAT3 [52].

3.7 | Concluding remarks

MS-based proteomics is a powerful tool for investigation of cellular phosphorylation patterns. Rikova et al. reported in 2007 a comprehensive proteomic profiling of 41 NSCLC cell lines and over 150 NSCLC tumors expressing different oncogenic kinases. This landmark study established the role of phosphorylation signaling and oncogenic kinase fusions in lung cancer. Genomic investigations that have been performed in the last 15 years confirmed their findings and identified oncogenic kinase fusions in approximately 5–10% of patients with LADC. Rapid translation of these findings has since then led to the approval of specific kinase inhibitors that are effective for treatment of patients with tumors harboring kinase fusions.

Despite this importance, the phosphorylation patterns induced by different oncogenic kinase fusions were not systematically investigated in a controlled cellular model system. In this study, we employed quantitative MS-based proteomics to comparatively analyze the phosphorylation patterns induced by exogenous expression of the oncogenic tyrosine kinase fusions EML4-ALK, KIF5B-ALK, KIF5B-RET, CD74-ROS1, and SDC4-ROS1 that are frequently found in patients with LADC. Our analyses demonstrate that all investigated kinase fusion induce widespread tyrosine phosphorylation and reveal that the kinase part primarily defines the induced phosphorylation patterns. However, we could also identify phosphorylation events that are likely specific to the fusion partner and might contribute to the subtle phenotypical differences observed in the clinic. The acquired phosphoproteomics dataset might serve as a useful resource for future studies focused on the effects of the kinase fusions in lung adenocarcinoma.

ACKNOWLEDGMENTS

The support of the IMB Microscopy Core Facility is gratefully acknowledged. Petra Beli was supported by the Emmy Noether Program (BE 5342/1-1). Sebastian A. Wagner was supported by the LOEWE program Ubiquitin Networks (Ub-Net) of the State of Hesse (Germany), the Else Kröner-Fresenius-Stiftung (2015_A124) and the Else

Kröner-Forschungskolleg Frankfurt. The usage of Proteomics and Microscopy core facilities at IMB is gratefully acknowledged.

Open access funding enabled and organized by Projekt DEAL.

CONFLICT OF INTEREST

The authors declare no conflict of interest.

AUTHOR CONTRIBUTIONS

Sebastian A. Wagner and Petra Beli designed and supervised the research. Sebastian A. Wagner, Andrea Voigt and Pawel P. Szczesniak performed experiments. Sebastian A. Wagner, Petra Beli and Justus F. Gräf analyzed the data. Sebastian A. Wagner and Petra Beli wrote the manuscript. All authors read and commented on the manuscript.

DATA AVAILABILITY STATEMENT

The mass spectrometry proteomics data have been deposited to the ProteomeXchange Consortium (http://proteomecentral.proteomexchange.org) via the PRIDE partner repository [53] with the dataset identifier PXD021904.

ORCID

Sebastian A. Wagner https://orcid.org/0000-0002-8629-6310
Petra Beli https://orcid.org/0000-0001-9507-9820

REFERENCES

1. Cancer Genome Atlas Research Network. Collisson, E. A., Campbell, J. D., Brooks, A. N., Berger, A. H., Lee, W., Chmielecki, J., Beer, D. G., Leslie, Cope, Creighton, C. J., Danilova, L., Ding, Li, Getz, G., Hammerman, P. S., Hayes, D. N., Hernandez, B., Herman, J. G., Heymach, J. V., Jurisica, I., Kucherlapati, R., … Tsao, M.-S. (2014). Comprehensive molecular profiling of lung adenocarcinoma. *Nature*, *511*, 543–550.
2. Cancer Genome Atlas Research Network. Hammerman, P. S., Lawrence, M. S., Voet, D., Jing, R., Cibulskis, K., Sivachenko, A., Stojanov, P., McKenna, A., Lander, E. S., Gabriel, S., Getz, G., Sougnez, C., Imielinski, M., Helman, E., Hernandez, B., Pho, N. H., Meyerson, M., Chu, A., Chun, H.-J. E., … Thomson, E.. (2012). Comprehensive genomic characterization of squamous cell lung cancers. *Nature*, *489*, 519–525.
3. Chen, B., Jiang, Lu, Zhong, M.-L., Li, J.-F., Li, B.-S., Peng, Li.-J, Dai, Yu.-T, Cui, Bo.-W, Yan, T.-Qi, Zhang, W.-Na, Weng, X.-Q., Xie, Y.-Y., Lu, J., Ren, R.-B., Chen, Su.-N, Hu, J.-Da, Wu, De.-P, Chen, Z., Tang, J.-Y., … Chen, S.-J. (2018). Identification of fusion genes and characterization of transcriptome features in T-cell acute lymphoblastic leukemia. *Proceedings of the National Academy of Sciences of the United States of America*, *115*, 373–378.
4. Branford, S., Wang, P., Yeung, D. T., Thomson, D., Purins, A., Wadham, C., Shahrin, N. H., Marum, J. E., Nataren, N., Parker, W. T., Geoghegan, J., Feng, J., Shanmuganathan, N., Mueller, M. C., Dietz, C., Stangl, D., Donaldson, Z., Altamura, H., Georgievski, J., … Hughes, T. P. (2018). Integrative genomic analysis reveals cancer-associated mutations at diagnosis of CML in patients with high-risk disease. *Blood*, *132*, 948–961.
5. Calvayrac, O., Pradines, A., Pons, E., Mazières, J., & Guibert, N. (2017). Molecular biomarkers for lung adenocarcinoma. *European Respiratory Journal*, *49*, 1601734.
6. Cancer Genome Atlas Research Network, Agrawal, N., Akbani, R., Aksoy, B. A., Ally, A., Arachchi, H., Asa, S. L., Auman, J. T., Balasundaram, M., Balu, S., Baylin, S. B., Behera, M., Bernard, B., Beroukhim, R., Bishop, J. A., Black, A. D., Bodenheimer, T., Boice, L., Bootwalla, M. S., Bowen, J., … Zou, L.. (2014). Integrated genomic characterization of papillary thyroid carcinoma. *Cell*, *159*, 676–90.
7. Cancer Genome Atlas Research Network (2013). Genomic and epigenomic landscapes of adult de novo acute myeloid leukemia. *New England Journal of Medicine*, *368*, 2059-2074.
8. Schram, A. M., Chang, M. T., Jonsson, P., & Drilon, A. (2017). Fusions in solid tumours: Diagnostic strategies, targeted therapy, and acquired resistance. *Nature Reviews Clinical Oncology*, *14*, 735-748.
9. Soda, M., Choi, Y. L., Enomoto, M., Takada, S., Yamashita, Y., Ishikawa, S., Fujiwara, S.-I., Watanabe, H., Kurashina, K., Hatanaka, H., Bando, M., Ohno, S., Ishikawa, Y., Aburatani, H., Niki, T., Sohara, Y., Sugiyama, Y., & Mano, H. (2007). Identification of the transforming EML4â"ALK fusion gene in non-small-cell lung cancer. *Nature*, *448*, 561–566.
10. Richards, M. W., O'regan, L., Roth, D., Montgomery, J. M., Straube, A., Fry, A. M., & Bayliss, R. (2015). Microtubule association of EML proteins and the EML4-ALK variant 3 oncoprotein require an N-terminal trimerization domain. *Biochemical Journal*, *467*, 529-536.
11. Takeuchi, K., Choi, Y. L., Togashi, Y., Soda, M., Hatano, S., Inamura, K., Takada, S., Ueno, T., Yamashita, Y., Satoh, Y., Okumura, S., Nakagawa, K., Ishikawa, Y., & Mano, H. (2009). KIF5B-ALK, a novel fusion oncokinase identified by an immunohistochemistry-based diagnostic system for ALK-positive lung cancer. *Clinical Cancer Research*, *15*, 3143-3149.
12. Kohno, T., Ichikawa, H., Totoki, Y., Yasuda, K., Hiramoto, M., Nammo, T., Sakamoto, H., Tsuta, K., Furuta, K., Shimada, Y., Iwakawa, R., Ogiwara, H., Oike, T., Enari, M., Schetter, A. J., Okayama, H., Haugen, A., Skaug, V., Chiku, S., … Shibata, T. (2012). KIF5B-RET fusions in lung adenocarcinoma. *Nature Medicine*, 375-377.
13. Bergethon, K., Shaw, A. T., Ignatius Ou, S.-H., Katayama, R., Lovly, C. M., Mcdonald, N. T., Massion, P. P., Siwak-Tapp, C., Gonzalez, A., Fang, R., Mark, E. J., Batten, J. M., Chen, H., Wilner, K. D., Kwak, E. L., Clark, J. W., Carbone, D. P., Ji, H., Engelman, J. A., … Iafrate, A. J (2012). *ROS1* rearrangements define a unique molecular class of lung cancers. *Journal of Clinical Oncology*, *30*, 863–870.
14. Kohno, T., Nakaoku, T., Tsuta, K., Tsuchihara, K., Matsumoto, S., Yoh, K., & Goto, K. (2015). Beyond ALK-RET, ROS1 and other oncogene fusions in lung cancer. *Translational Lung Cancer Research*, *4*, 156–64.
15. Kwak, E. L., Bang, Y.-J., Camidge, D. R, Shaw, A. T., Solomon, B., Maki, R. G., Ou, S.-H. I., Dezube, B. J., Jänne, P. A., Costa, D. B., Varella-Garcia, M., Kim, W.-Ho, Lynch, T. J., Fidias, P., Stubbs, H., Engelman, J. A., Sequist, L. V., Tan, W., Gandhi, L., … Iafrate, A. J (2010). Anaplastic lymphoma kinase inhibition in Nonâ"small-cell lung cancer. *New England Journal of Medicine*, *363*, 1693–1703.
16. Shaw, A. T., Ou, S.-H. I., Bang, Y.-J., Camidge, D. R, Solomon, B. J., Salgia, R., Riely, G. J., Varella-Garcia, M., Shapiro, G. I., Costa, D. B., Doebele, R. C., Le, L. P., Zheng, Z., Tan, W., Stephenson, P., Shreeve, S. M, Tye, L. M., Christensen, J. G., Wilner, K. D., … Iafrate, A. J (2014). Crizotinib in ROS1 -rearranged Nonâ"small-cell lung cancer. *New England Journal of Medicine*, *371*, 1963–1971.
17. Harjes, P., & Wanker, E. E. (2003). The hunt for huntingtin function: Interaction partners tell many different stories. *Trends in Biochemical Sciences*, *28*, 425–433.
18. Shaw, A. T., Kim, D. W., Mehra, R., Tan, D. S., Felip, E., Chow, L. Q., Camidge, D. R., Vansteenkiste, J., Sharma, S., De Pas, T., Riely, G. J., Solomon, B. J., Wolf, J., Thomas, M., Schuler, M., Liu, G., Santoro, A., Lau, Y. Y., Goldwasser M., … Engelman, J. A.. (2014). Ceritinib in ALK-rearranged non-small-cell lung cancer. *New England Journal of Medicine*, *370*(13):1189-97.
19. Drilon, A., Oxnard, G. R., Tan, D. S. W., Loong, H. H. F., Johnson, M., Gainor, J., Mccoach, C. E., Gautschi, O., Besse, B., Cho, B. C., Peled, N., Weiss, J., Kim, Yu-J, Ohe, Y., Nishio, M., Park, K., Patel, J., Seto, T., Sakamoto, T., … Subbiah, V. (2020). Efficacy of Selpercatinib in RET fusionâ"positive Nonâ"small-cell lung cancer. *New England Journal of Medicine*, 813-824.
20. Larance, M., & Lamond, A. I. (2015). Multidimensional proteomics for cell biology. *Nature Reviews Molecular Cell Biology*, *16*, 269-280.

21. Choudhary, C., & Mann, M. (2010). Decoding signalling networks by mass spectrometry-based proteomics. *Nature Reviews Molecular Cell Biology*, *11*, 427-439.
22. Sabidó, E., Selevsek, N., & Aebersold, R. (2012). Mass spectrometry-based proteomics for systems biology. *Current Opinion in Biotechnology*, *23*, 591-597.
23. Altelaar, A. F. M, Munoz, J., & Heck, A. J. R. (2013). Next-generation proteomics: Towards an integrative view of proteome dynamics. *Nature Reviews Genetics*, *14*, 35–48.
24. Beli, P., Lukashchuk, N., Wagner, S. A., Weinert, B. T., Olsen, J. V., Baskcomb, L., Mann, M., Jackson, S. P., & Choudhary, C. (2012). Proteomic investigations reveal a role for RNA processing factor THRAP3 in the DNA damage response. *Molecular Cell*, *46*, 212-225.
25. Bensimon, A., Schmidt, A., Ziv, Y., Elkon, R., Wang, S.-Y., Chen, D. J., Aebersold, R., & Shiloh, Y. (2010). ATM-dependent and -independent dynamics of the nuclear phosphoproteome after DNA damage. *Science Signaling*, *3*, rs3.
26. Matsuoka, S., Ballif, B. A., Smogorzewska, A., Mcdonald, E. R., Hurov, K. E., Luo, J., Bakalarski, C. E., Zhao, Z., Solimini, N., Lerenthal, Y., Shiloh, Y., Gygi, S. P., & Elledge, S. J. (2007). ATM and ATR substrate analysis reveals extensive protein networks responsive to DNA damage. *Science*, *316*, 1160-1166.
27. Bennetzen, M. V., Larsen, D. H., Bunkenborg, J., Bartek, J., Lukas, J., & Andersen, J. S. (2010). Site-specific phosphorylation dynamics of the nuclear proteome during the DNA damage response. *Molecular and Cellular Proteomics*, *9*, 1314-1323.
28. Blasius, M., Forment, J. V., Thakkar, N., Wagner, S. A., Choudhary, C., & Jackson, S. P. (2011). A phospho-proteomic screen identifies substrates of the checkpoint kinase Chk1. *Genome Biology*, *12*, R78.
29. Stokes, M. P., Rush, J., Macneill, J., Ren, J. M., Sprott, K., Nardone, J., Yang, V., Beausoleil, S. A., Gygi, S. P., Livingstone, M., Zhang, H., Polakiewicz, R. D., & Comb, M. J. (2007). Profiling of UV-induced ATM/ATR signaling pathways. *Proceedings of the National Academy of Sciences of the United States of America*, *104*, 19855–19860.
30. Rikova, K., Guo, A., Zeng, Q., Possemato, A., Yu, J., Haack, H., Nardone, J., Lee, K., Reeves, C., Li, Yu, Hu, Y., Tan, Z., Stokes, M., Sullivan, L., Mitchell, J., Wetzel, R., Macneill, J., Ren, J. M., Yuan, J., … Comb, M. J. (2007). Global survey of phosphotyrosine signaling identifies oncogenic kinases in lung cancer. *Cell*, 1190-1203.
31. Ong, S.-En, Blagoev, B., Kratchmarova, I., Kristensen, D. B., Steen, H., Pandey, A., & Mann, M. (2002). Stable isotope labeling by amino acids in cell culture, SILAC, as a simple and accurate approach to expression proteomics. *Molecular and Cellular Proteomics*, *1*, 376–386.
32. Borisova, M. E., Wagner, S. A., Beli, P. (Eds:) Methods in Molecular Biology, *1599*, Humana Press, New York 2017. *ATM Kinase*. Mass Spectrometry-Based Proteomics for Quantifying DNA Damage-Induced Phosphorylation.
33. Michalski, A., Damoc, E., Hauschild, J.-P., Lange, O., Wieghaus, A., Makarov, A., Nagaraj, N., Cox, J., Mann, M., & Horning, S. (2011). Mass spectrometry-based proteomics using Q exactive, a high-performance benchtop quadrupole orbitrap mass spectrometer. *Molecular and Cellular Proteomics*, *10*, M111.011015.
34. Olsen, J. V., Macek, B., Lange, O., Makarov, A., Horning, S., & Mann, M. (2007). Higher-energy C-trap dissociation for peptide modification analysis. *Nature Methods*, *4*, 709-712.
35. Cox, J., & Mann, M. (2008). MaxQuant enables high peptide identification rates, individualized p.p.b.-range mass accuracies and proteome-wide protein quantification. *Nature Biotechnology*, *26*, 1367-1372.
36. Cox, Jü, Neuhauser, N., Michalski, A., Scheltema, R. A., Olsen, J. V., & Mann, M. (2011). Andromeda: A peptide search engine integrated into the MaxQuant environment. *Journal of Proteome Research*, *10*, 1794-1805.
37. Olsen, J. V., Blagoev, B., Gnad, F., Macek, B., Kumar, C., Mortensen, P., & Mann, M. (2006). Global, in vivo, and site-specific phosphorylation dynamics in signaling networks. *Cell*, *127*, 635-648.
38. Elias, J. E., & Gygi, S. P. (2007). Target-decoy search strategy for increased confidence in large-scale protein identifications by mass spectrometry. *Nature Methods*, *4*, 207-214.
39. Ritchie, M. E., Phipson, B., Wu, Di, Hu, Y., Law, C. W., Shi, W., & Smyth, G. K. (2015). Limma powers differential expression analyses for RNA-sequencing and microarray studies. *Nucleic Acids Research*, *43*, e47-e47.
40. Casado, P., Rodriguez-Prados, J.-C., Cosulich, S. C., Guichard, S., Vanhaesebroeck, B., Joel, S., & Cutillas, P. R. (2013). Kinase-substrate enrichment analysis provides insights into the heterogeneity of signaling pathway activation in leukemia cells. *Science Signaling*, *6*, rs6-rs6.
41. Wiredja, D. D., Koyutürk, M., & Chance, M. R. (2017). The KSEA App: a web-based tool for kinase activity inference from quantitative phosphoproteomics. *Bioinformatics*, *33*, 3489–3491.
42. Hornbeck, P. V., Kornhauser, J. M., Tkachev, S., Zhang, B., Skrzypek, E., Murray, B., Latham, V., & Sullivan, M. (2012). PhosphoSitePlus: A comprehensive resource for investigating the structure and function of experimentally determined post-translational modifications in man and mouse. *Nucleic Acids Research*. *40*(Database issue):D261-70.
43. Linding, R., Jensen, L. J., Ostheimer, G. J., Van Vugt, M. A. T. M., Jørgensen, C., Miron, I. M., Diella, F., Colwill, K., Taylor, L., Elder, K., Metalnikov, P., Nguyen, V., Pasculescu, A., Jin, J., Park, J. G., Samson, L. D., Woodgett, J. R., Russell, R. B., Bork, P., … van Vugt, M. A. T. M. (2007). Systematic discovery of in vivo phosphorylation networks. *Cell*, *129*, 1415–1426.
44. Krug, K., Mertins, P., Zhang, B., Hornbeck, P., Raju, R., Ahmad, R., Szucs, M., Mundt, F., Forestier, D., Jane-Valbuena, J., Keshishian, H., Gillette, M. A., Tamayo, P., Mesirov, J. P., Jaffe, J. D., Carr, S., & Mani, D. R. (2019). A curated resource for phosphosite-specific signature analysis. *Molecular and Cellular Proteomics*, *18*, 576–593.
45. Forbes, S. A., Beare, D., Boutselakis, H., Bamford, S., Bindal, N., Tate, J., Cole, C. G., Ward, S., Dawson, E., Ponting, L., Stefancsik, R., Harsha, B., Kok, C. Y., Jia, M., Jubb, H., Sondka, Z., Thompson, S., De, T., & Campbell, P. J. (2017). COSMIC: Somatic cancer genetics at high-resolution. *Nucleic Acids Research*. *45*, D777–D783.
46. Kohno, T., Ichikawa, H., Totoki, Y., Yasuda, K., Hiramoto, M., Nammo, T., Sakamoto, H., Tsuta, K., Furuta, K., Shimada, Y., Iwakawa, R., Ogiwara, H., Oike, T., Enari, M., Schetter, A. J., Okayama, H., Haugen, A., Skaug, V., Chiku, S., … Shibata, T. (2012). KIF5B-RET fusions in lung adenocarcinoma. *Nature Medicine*, *18*, 375–377.
47. Jun, H. J., Johnson, H., Bronson, R. T., De Feraudy, S., White, F., & Charest, A. (2012). The oncogenic lung cancer fusion kinase CD74-ROS activates a novel invasiveness pathway through E-Syt1 phosphorylation. *Cancer Research*, *72*, 3764-3774.
48. Chiarle, R., Simmons, W. J., Cai, H., Dhall, G., Zamo, A., Raz, R., Karras, J. G., Levy, D. E., & Inghirami, G. (2005). Stat3 is required for ALK-mediated lymphomagenesis and provides a possible therapeutic target. *Nature Medicine*, 623-629.
49. Qian, Y., Chai, S., Liang, Z., Wang, Y., Zhou, Y., Xu, X., Zhang, C., Zhang, M., Si, J., Huang, F., Huang, Z., Hong, W., & Wang, K. (2014). KIF5B-RET fusion kinase promotes cell growth by multilevel activation of STAT3 in lung cancer. *Molecular Cancer [Electronic Resource]*, *13*, 176.
50. Crescenzo, R., Abate, F., Lasorsa, E., Tabbo', F., Gaudiano, M., Chiesa, N., Di Giacomo, F., Spaccarotella, E., Barbarossa, L., Ercole, E., Todaro, M., Boi, M., Acquaviva, A., Ficarra, E., Novero, D., Rinaldi, A., Tousseyn, T., Rosenwald, A., Kenner, L., … Inghirami, G. (2015). Convergent mutations and kinase fusions lead to oncogenic STAT3 activation in anaplastic large cell lymphoma. *Cancer Cell*, *27*, 516–532.
51. Mcbride, K. M. (2002). Regulated nuclear import of the STAT1 transcription factor by direct binding of importin-alpha. *Embo Journal*, *21*, 1754-1763.
52. Darnell, J. E. Jr. (1997). STATs and gene regulation. *Science*, *277*(5332), 1630-1635.
53. Perez-Riverol, Y., Csordas, A., Bai, J., Bernal-Llinares, M., Hewapathirana, S., Kundu, D. J., Inuganti, A., Griss, J., Mayer, G., Eisenacher, M.,

Pérez, E., Uszkoreit, J., Pfeuffer, J., Sachsenberg, T., Yilmaz, S., Tiwary, S., Cox, J., Audain, E., Walzer, M., … Vizcaíno, J. A.. (2019). The PRIDE database and related tools and resources in 2019: Improving support for quantification data. *Nucleic Acids Research*, *47*(D1):D442-D450.

SUPPORTING INFORMATION

Additional supporting information may be found online https://doi.org/10.1002/pmic.202000283 in the Supporting Information section at the end of the article.

How to cite this article: Wagner, S. A., Szczesniak, P. P., Voigt, A., Gräf, J. F., Beli, P. (2021). Proteomic analysis of tyrosine phosphorylation induced by exogenous expression of oncogenic kinase fusions identified in lung adenocarcinoma. *Proteomics*;*21*:e2000283.
https://doi.org/10.1002/pmic.202000283